

# Bipolar electrodeposition of organic electrochemical transistor arrays

*Jianlong Ji<sup>a</sup>, Yinpeng Fu<sup>a</sup>, Jingxiao Wang<sup>a</sup>, Po-Yu Chen<sup>b</sup>, Dan Han<sup>a</sup>, Qiang Zhang<sup>a</sup>, Wendong  
Zhang<sup>a</sup>, Shengbo Sang<sup>\*a</sup>, Xing Yang<sup>\*c</sup>, Zhengdong Cheng<sup>\*d,e</sup>*

*<sup>a</sup> MicroNano System Research Center, College of Information and Computer & Key Laboratory of  
Advanced Transducers and Intelligent Control System of Ministry of Education and Shanxi  
Province, Taiyuan University of Technology, Taiyuan, 030024, PRC*

*<sup>b</sup> Department of Medicinal and Applied Chemistry, Kaohsiung Medical University, Kaohsiung 807,  
Taiwan, ROC*

*<sup>c</sup> The State Key Laboratory of Precision Measurement Technology and Instruments, Department of  
Precision Instrument, Tsinghua University, Beijing 100084, PRC*

*<sup>d</sup> Artie McFerrin Department of Chemical Engineering, Texas A&M University, College Station,  
TX 77843-3122, USA*

*<sup>e</sup> Department of Chemical Engineering, Texas A&M University at Qatar, PO Box 23874, Doha,  
Qatar*

## The experimental setup and characterizations

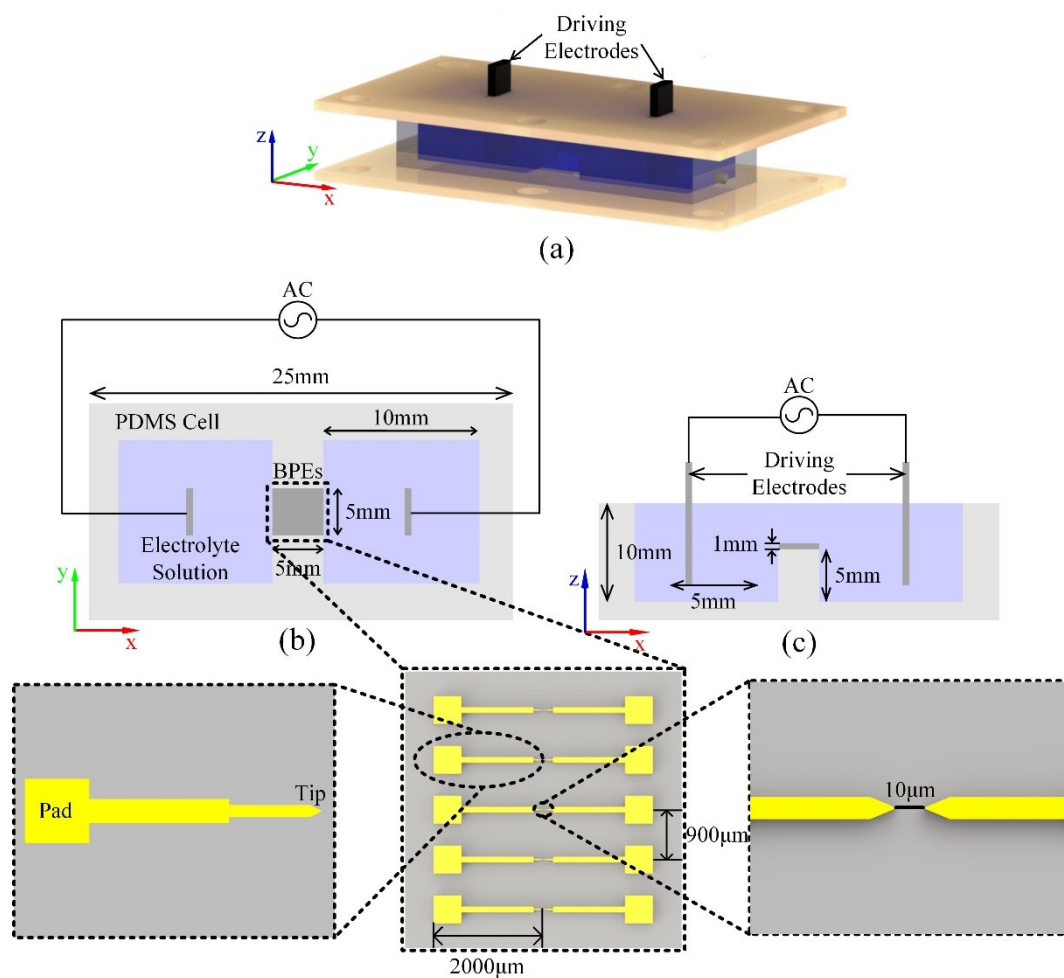


Figure S1. Illustrations of the experimental setup for alternating current bipolar electrodepositions (AC-BED). (a) The scheme of the microfluidic chip. (b) Dimensions in the top view. (c) Dimensions in the side view.

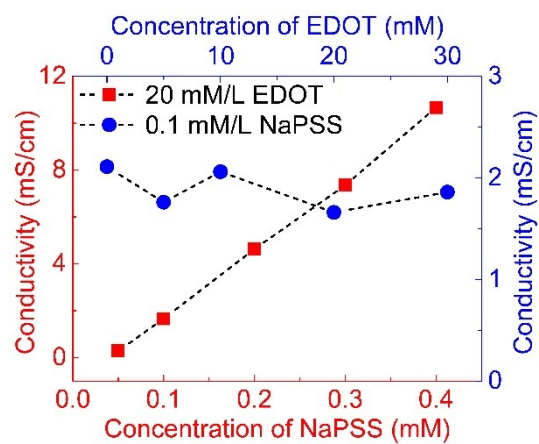


Figure S2. Electrolyte conductivities versus the concentration of EDOT and NaPSS. Red squares were obtained by fixing the concentration of EDOT at  $2 \times 10^4 \mu\text{M}$ . Blue circles were obtained by fixing the concentration of NaPSS at  $10^2 \mu\text{M}$ . The dashed lines are guides to aid visualization.

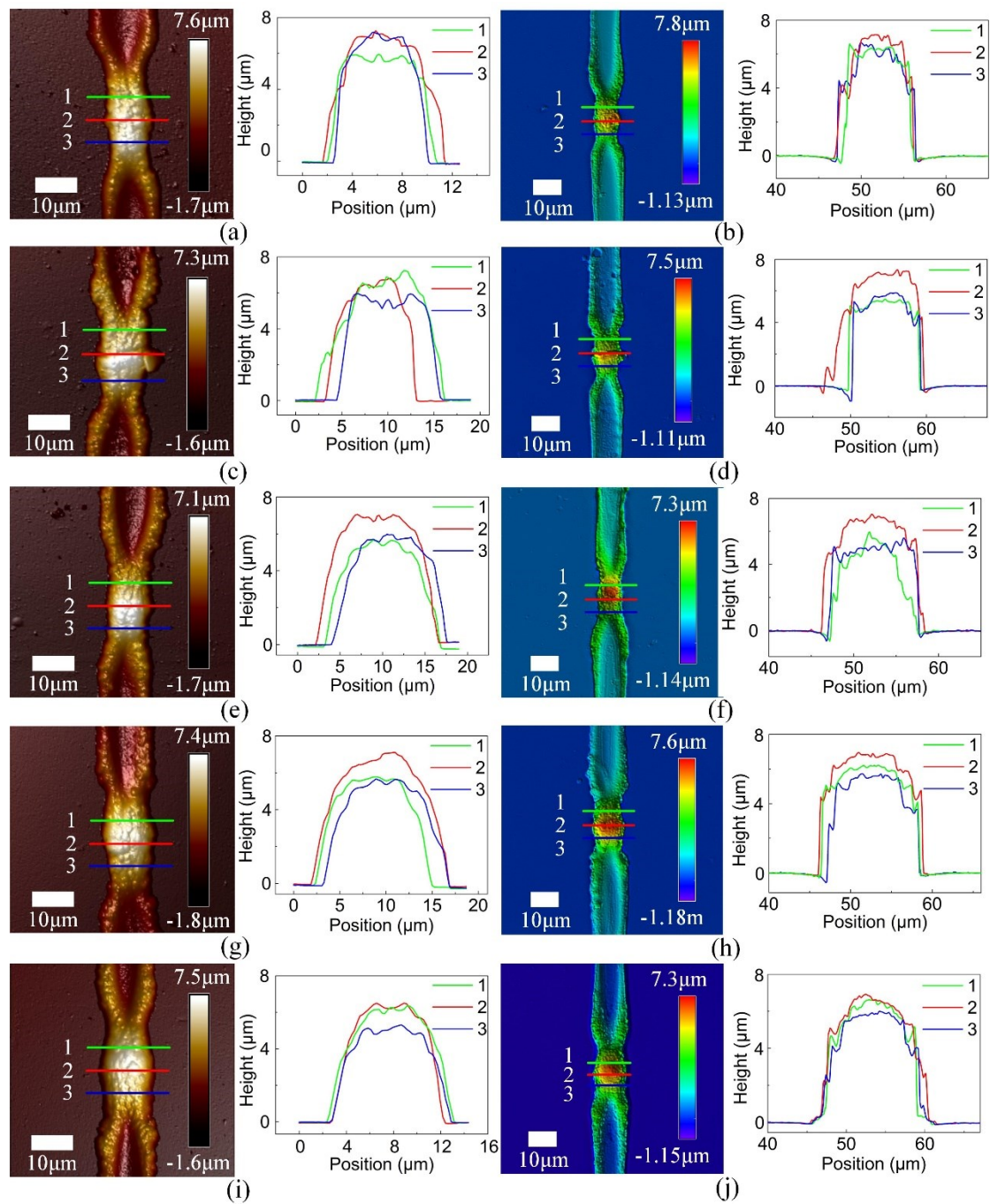


Figure S3. Film morphologies and profiles obtained by the atomic force microscope (AFM) and the laser confocal scanning microscope (LCSM).

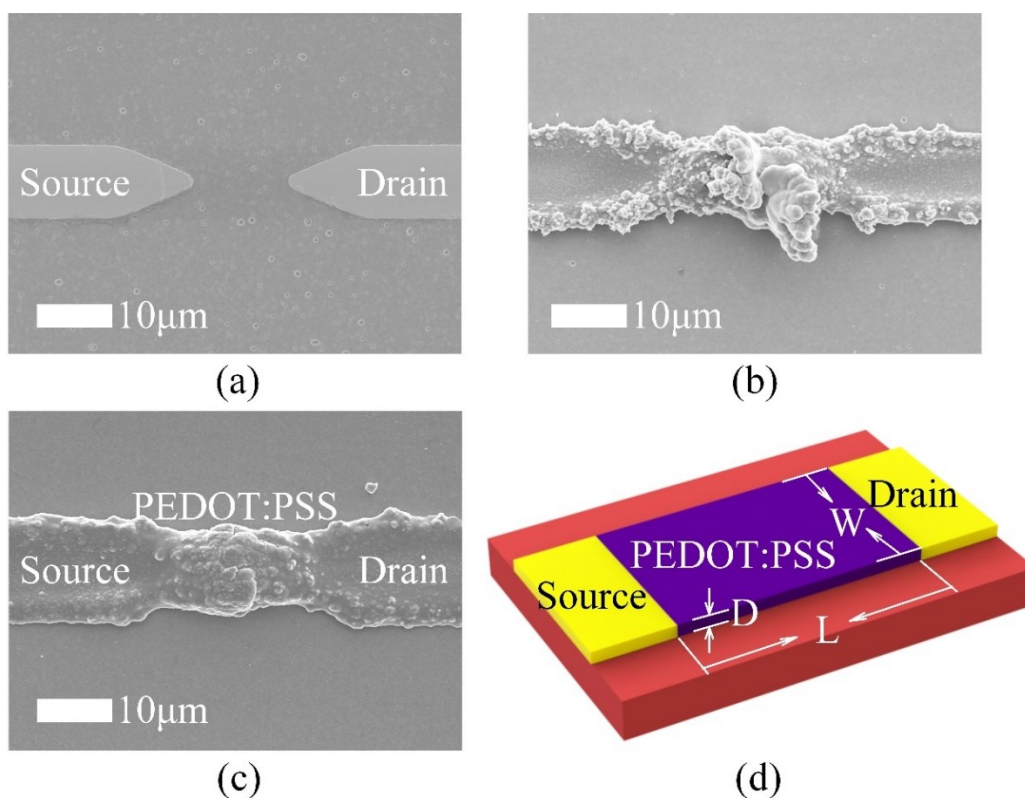


Figure S4. Morphologies of electrodes and electrodeposited films. (a) The scanning electron microscope (SEM) image of electrodes without electrodeposition. (b) and (c) SEM images of electrodes electrodeposited with PEDOT:PSS films. The preparation parameter for (b) was  $16 V_{p-p}$  at 20 Hz (undesired); for (c)  $16 V_{p-p}$  at 50 Hz; (d) The definitions of  $W$  and  $D$  of PEDOT:PSS layer.

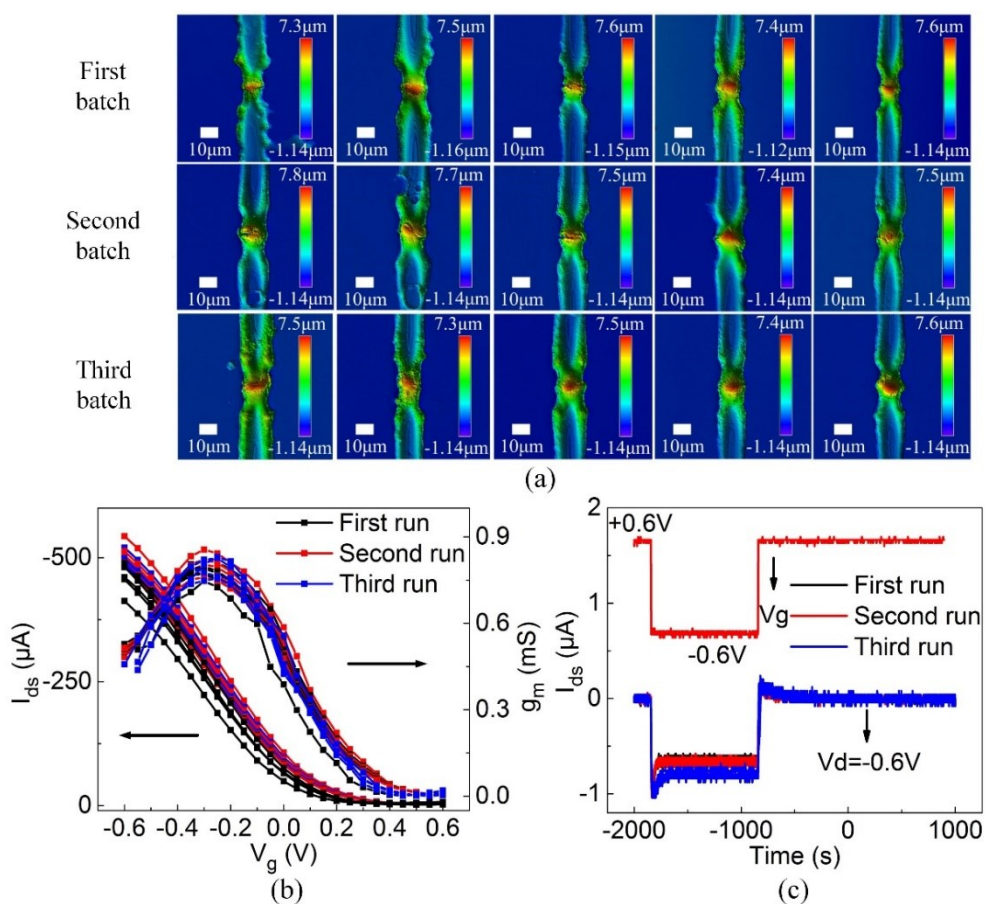


Figure S5. Semiconducting films fabricated by AC-BED in three batches. (a) The LSCM images. (b) The transfer and transconductance curves. (c) The transient responses.

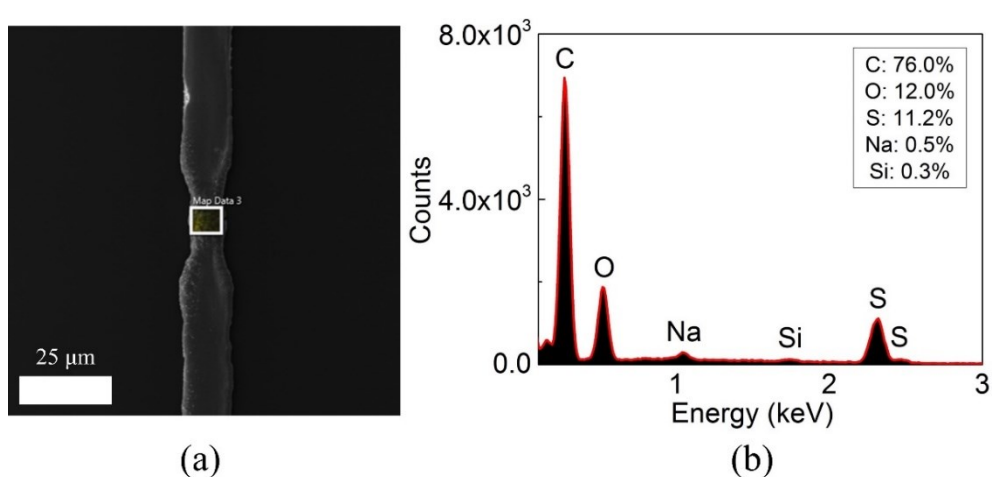


Figure S6. The elemental analysis of as-prepared PEDOT:PSS film, which indicates the residual of sodium cations. (a) The SEM image. (b) The energy dispersive spectrometry spectrum.

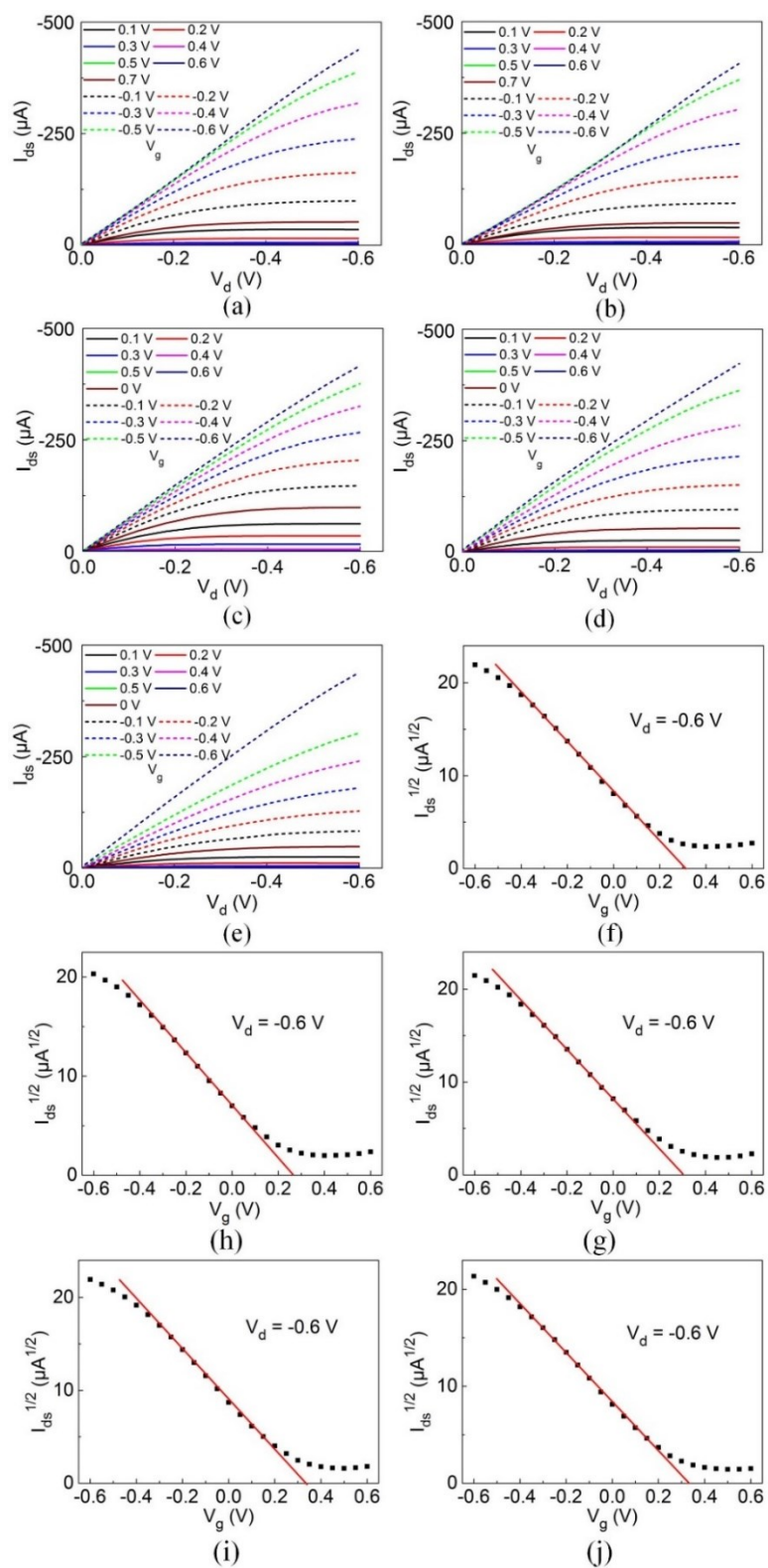


Figure S7. Steady-state characteristic curves of OECTs. The output curves (a–e) and the diagrams of  $I_{ds}^{1/2}$  versus  $V_g$  (f–j) of five transistors fabricated in the first run. The corresponding film morphologies and profiles are shown in Figures 2(b) and S3.

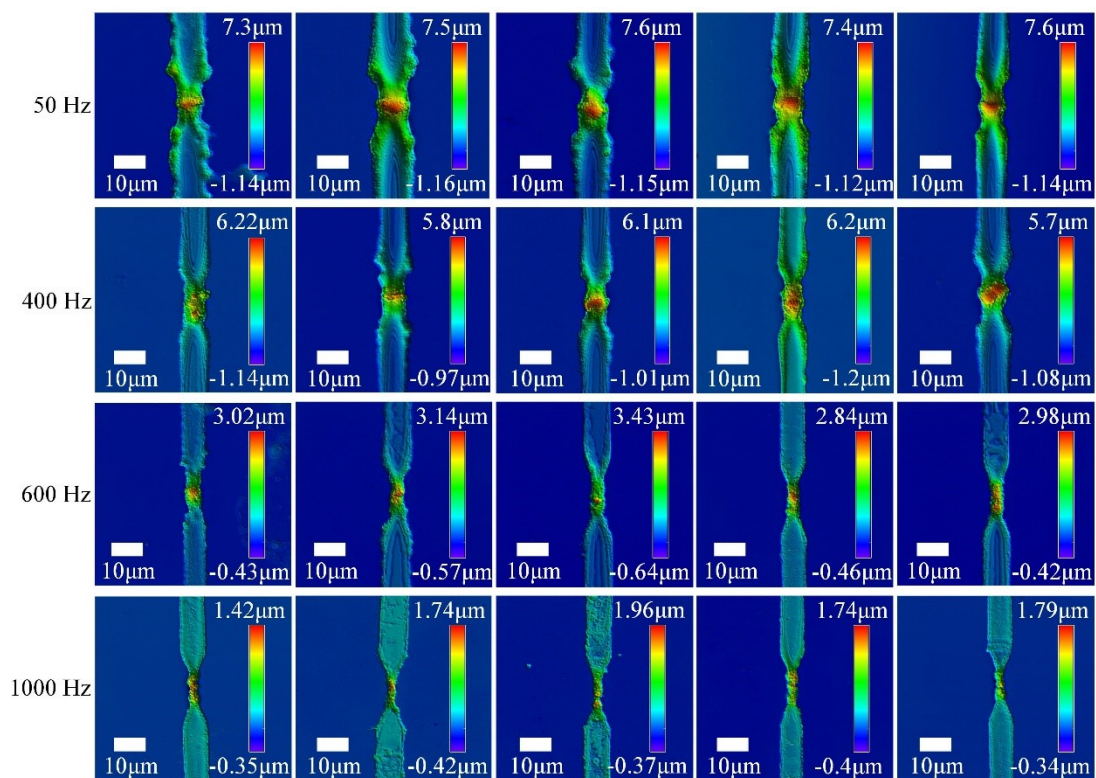


Figure S8. The LSCM image of PEDOT:PSS films prepared by different frequencies. The geometry parameters are reported in Figure 3(a).

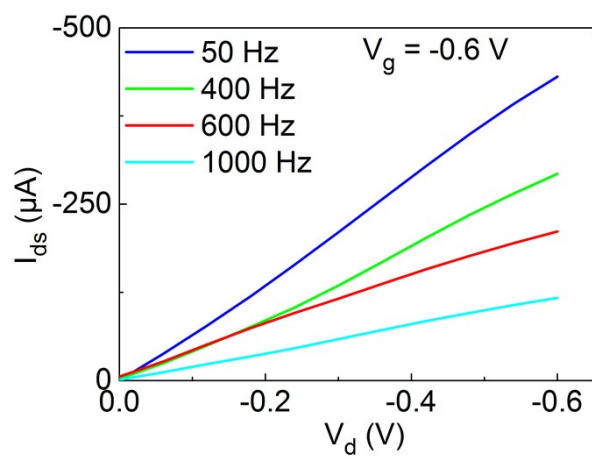


Figure S9. The output characteristic curve of OECTs ( $V_g = -0.6V$ ) which was prepared using different frequencies.



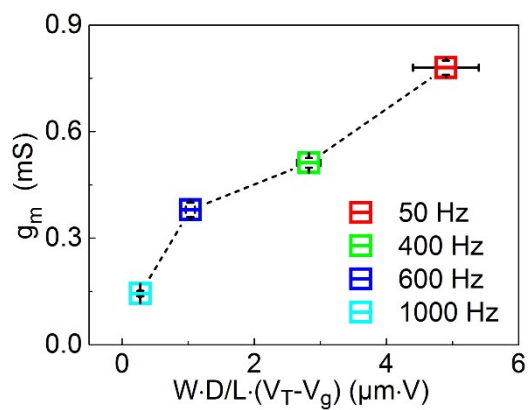


Figure S10. According to the Bernards-Malliaras model<sup>1,2</sup>,  $g_m$  of the OECT could be represented as  $\mu \cdot C^* \cdot W \cdot D/L \cdot (V_T - V_g)$  in the saturation region. Thus,  $\mu \cdot C^*$  can be obtained by fitting the diagram of  $g_m$  versus  $W \cdot D/L \cdot (V_T - V_g)$ . Here, the fitting result of  $\mu \cdot C^*$  was  $1.3 \pm 0.1 \text{ Fcm}^{-1}\text{V}^{-1}\text{S}^{-1}$ .

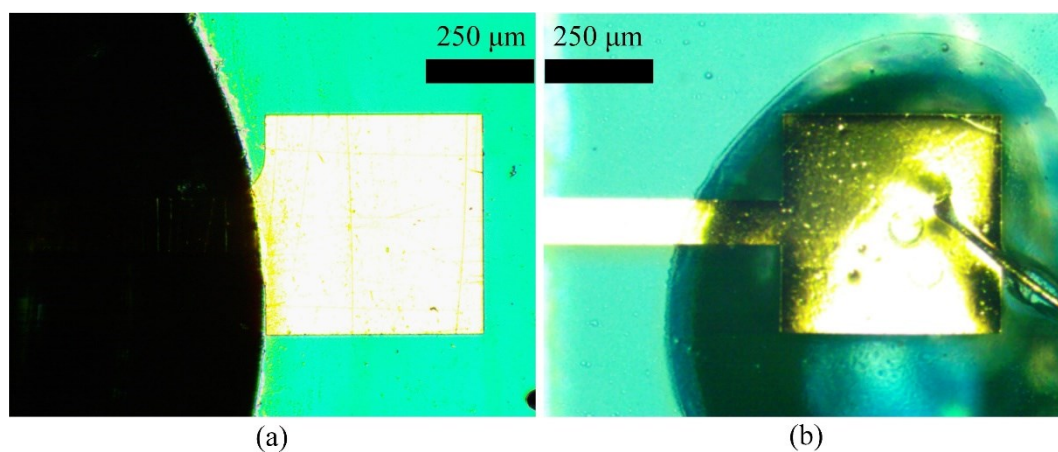


Figure S11. Using the UV-sensitive glue to define the exposure area for electrochemical impedance spectrum (EIS) tests. (a) The target area is a pad. (b) The target area is a tip.

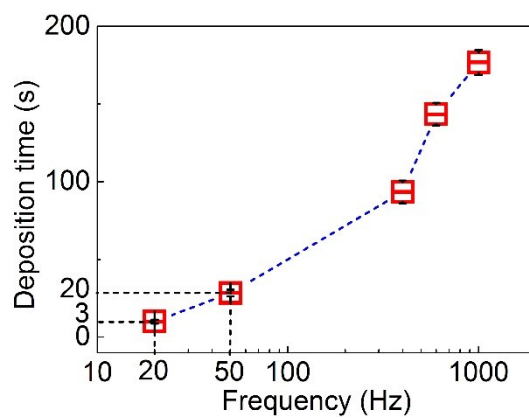


Figure S12. The plot of the deposition time versus the AC frequency,  $n=3$  for the standard error bar.

Table S1. The fitting results of Figure 4(a)–4(c).

	$R_s$ ( $\Omega$ )	$R_{ct}$ ( $\Omega$ )	$Q$ ( $FS^{(\alpha-1)}$ )	$\alpha$	$C_{eff}$ (F)
<b>Electrolyte/Driving electrode</b>	28	$6.5 \times 10^4$	$3.3 \times 10^{-5}$	0.7	$4.5 \times 10^{-6}$
<b>Electrolyte/BPE pad</b>	14	$6.9 \times 10^4$	$2.2 \times 10^{-5}$	0.9	$9.0 \times 10^{-6}$
<b>Electrolyte/BPE tip</b>	24	$2.9 \times 10^5$	$1.6 \times 10^{-5}$	0.85	$4.0 \times 10^{-6}$

**REFERENCE:**

1. J. T. Friedlein, R. R. McLeod and J. Rivnay, *Organic Electronics*, 2018, **63**, 398-414.
2. D. A. Bernards and G. G. Malliaras, *Advanced Functional Materials*, 2007, **17**, 3538-3544.